# On Energy Transfer and Dissipation of Intruder Impacting Granular Materials based on Discrete Element Simulations

Shaomin Liang[1]*, Y. T. Feng[2], Tingting Zhao[1], Zhihua Wang[1]

1. College of Mechanical and Vehicle Engineering, Taiyuan University of Technology, Taiyuan 030024, China
2. Zienkiewicz Centre for Computational Engineering, Swansea University, Swansea SA1 8EP, UK

*Corresponding author: shmliang@163.com

Tel: +8619969306766

**Abstract:** The impact process of a rigid intruder on granular materials can reveal some fundamental physical phenomena related to granular materials. Most existing investigations on impact problems of granular materials are mainly focused on the phenomenological description of the impact process without comprehensive understanding of energy dispersion of granular materials. In this paper, the discrete element method (DEM) is adopted to investigate the impact process of granular materials subject to an intruder. The kinetic and potential energy of the intruder is transferred to granular materials through the contact surface during impact. The granular material achieves dynamic equilibrium at the macroscopic level. The results reveal that the momentum transfer is typically radial at the collision point, indicating that the friction between particles and the intruder is not crucial. The shape and size of intruder significantly affects the energy transfer and the contact area between intruder and granular material. There is a quantitative relationship between the proportion of granular material involved in energy dissipation, the dissipation time and the energy transferred to the granular system, particularly when the granular system is sufficiently large.

**Keywords:** dynamic impact; granular material; intruder shape; energy dissipation; discrete element method

## 1. Introduction

Impact and collision are ubiquitous phenomena involved in discrete systems in nature, from molecular interactions to planetary collisions [1-4]. The impact of a solid intruder can affect both the surface and internal structure of granular materials on micro-scale [5]. Normally, the impact can form a bowl-shaped crater on the granular bed and cause the spray of particles outwardly [6,7]. Recently, the impact phenomena including the crater shape, the impact depth, the dynamic response, the boundary effect and the filling block effect have been investigated by numerical simulations and physical experiments [8-11]. The formations of craters of granualr materials on Earth, Mars and other planets have also been considered under impact [12-14]. The depth and diameter of impact craters can indicate the formation of volcanoes and meteorite craters. Moreover, the energy transformation and dissipation during the impact process is also very important to understand the generation of crater in granular materials [15-17]. The energy dissipation can be better understood by considering collisions between particles at the micro-scale.

According to the different impact velocities, the impact process can be classified into quasi-static penetration, dynamic impact, high-speed impact and ultra-high-speed impact [18-20]. Dynamic impact is particularly useful for studying the physical properties of granular media as it more accurately reflects the collisions that occur in everyday life and production. The wave propagation process is closely linked to the impact process, and the analysis of energy is crucial [21-23]. In recent years, the impact depth, velocity variation and other related issues of intruders with specific kinetic energy in granular media have been extensively studied [6,24]. When dealing with low-speed impact with loose granular filling considers, the interaction between intruder and granular media is modeled as the sum of a depth-dependent linear friction force and inertial resistance, which is proportional to square of the velocity $v^2$ , and a static friction resistance that is proportional to the impact depth $z$ [12,25]. Poncelet [26,27] proposed the following dynamic impact equation: $Ma = Mg - h(z)v^2 - \beta(z)$ , where $M$ is the intruder mass and $g$ is the gravitational acceleration; $z$ is the impact depth, and $z = 0$ corresponds to the lower edge of the intruder contacting the upper surface of the granular bed; $\beta(z)$ is the quasi-static drag coefficient, which can be determined when short-term fluctuations are neglected. $\beta(z)$ is considered as a constant during dynamic impact. Consequently, $h(z)v^2$ plays a dominant role in the impact resistance [28] and is typically regarded as an inertia term that characterize the momentum and energy transfer from the intruder to the granular media [29,30]. The validity of the above equation has been confirmed in subsequent experimental studies, demonstrating its ability to describe the dynamic characteristics of the intruder.

According to the physical characteristics of granular media, different numerical models and methods are used for simulations. The discrete element method (DEM) has unique advantages in simulating granular media, while continuum-based models are better suited for strong and tough media or large planetary impacts[17,31-33]. In the study of granular properties, the focus is on the impact of cm-scale objects on granular media, while the continuum-based model is not suitable for granular media [34]. Therefore, DEM is one of the most effective numerical methods to simulate the dynamic behavior of granular materials with the loose and discontinuous nature [35]. At present, both two and three dimensional DEM have been applied to the numerical study of collisions of granular media in various fields [36,37].

In this study, DEM is used to simulate the impact of a solid intruder on a granular material. A non-linear contact model is adopted to describe the interaction between the spherical particles. Here the interaction between intruder and spherical particle are interpreted comprehensively. The process is analyzed in detail from the aspects of energy transfer, the influence of contact area and the energy dissipation of granular media.

## 2. Discrete element method for granular materials

### 2.1 Contact force between particles

Considering the structural characteristics of granular material and its dynamic response during collision and impact, the non-linear contact model is applied to account for the interaction between spherical particles treated as discrete elements. The particle shape has a certain impact on the impact process [38]. There are many researches on particle shape at present. In order to simplify the simulation, the spherical discrete element model is used in this paper. The contact force between two discrete elements, as shown in Fig.1(a) for two elements *i* and *j*, can be divided into two parts: the normal contact force $\boldsymbol{F}_\mathrm{n}$ and the tangential contact force $\boldsymbol{F}_\mathrm{s}$ , which can be represented by a spring-damper-slider phenomenological model as shown in Fig.1(b) and Fig.1(c), where $K_\mathrm{n}$ and $K_\mathrm{s}$ are the normal and tangential stiffnesses respectively; $C_\mathrm{n}$ and $C_\mathrm{s}$ are the normal and tangential damping coefficients; $\mu_\mathrm{n}$

is the inter-granular friction coefficient.

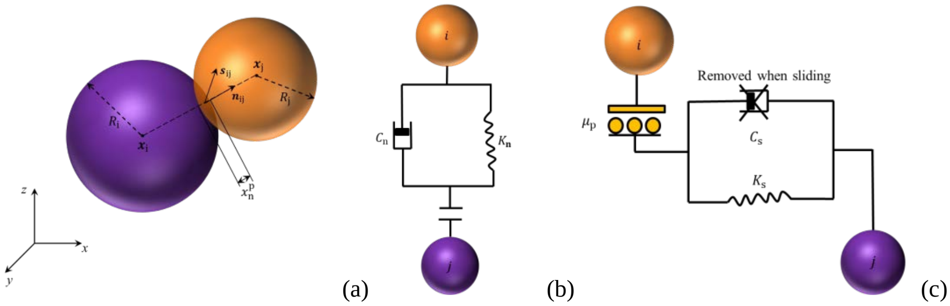


**Fig. 1** Contact model between two particles.

The normal overlap between the two elements $i$ and $j$ in contact is $x_{\mathrm{n}}^{\mathrm{p}} = R_i + R_j - d_{ij}$, here $d_{ij} = |\mathbf{x}_i - \mathbf{x}_j|$ is the distance between the centers of the two elements represented by $\mathbf{x}_i$ and $\mathbf{x}_j$ respectively; and $R_i$ and $R_j$ are their radii. Both normal and tangential contact forces include an elastic force and a viscous damping force, while the tangential force is limited based on the Coulomb friction modal. The two forces can be written as [39]:

$$\boldsymbol{F}_{\mathrm{n}} = (F_{\mathrm{ne}} + F_{\mathrm{nv}}) \cdot \mathbf{n}_{ij} \tag{1}$$

$$\boldsymbol{F}_{\mathrm{s}} = \min\left|(F_{\mathrm{se}} + F_{\mathrm{sv}}), \mu_{\mathrm{p}}|\boldsymbol{F}_{\mathrm{n}}|\right| \cdot \mathbf{s}_{ij} \tag{2}$$

where $\mu_{\mathrm{p}}$ is the friction coefficient between the two contacting particles; $\mathbf{n}_{ij}$ is the unit normal vector from the center of sphere $i$ to the center sphere $j$; and $\mathbf{s}_{ij}$ is the tangential vector between two particles. The Hertzian-Mindlin nonlinear contact model is applied to compute the elastic force between granular materials. In the normal direction, the forces between the two contacting particles include the Hertzian elastic force and non-linear viscous force [40], and the two forces can be written as

$$F_{\mathrm{ne}} = K_{\mathrm{n}}\left(x_{\mathrm{n}}^{\mathrm{p}}\right)^{3/2}$$

$$F_{\mathrm{nv}} = \frac{3}{2} A K_{\mathrm{n}}\left(x_{\mathrm{n}}^{\mathrm{p}}\right)^{1/2} \Delta \dot{x}_{\mathrm{n}}^{\mathrm{p}} \tag{3}$$

where $\dot{x}_{\mathrm{n}}^{\mathrm{p}}$ represents the relative velocity of the two contacting particles; $A$ is the viscous parameter of the granular material, which is related to the mechanical parameters, such as deformation modulus, viscous coefficient and Poisson's ratio, and can be determined with the resilience coefficient of granular collision at a certain velocity. The normal stiffness coefficient between the two contacting particles can be written as $K_{\mathrm{n}} = \frac{3}{4}E^*\sqrt{R^*}$, where $E^* = \frac{E}{2(1-v^2)}$, $R^* = \frac{R_iR_j}{R_i+R_j}$, here $E$ and $v$ are the elastic modulus and the Poisson's ratio of the granular material, respectively. Based on the Mindlin theory and ignoring the influence of viscous force, the tangential elastic force can be expressed as [41]

$$F_{\mathrm{se}} = K_{\mathrm{s}}\left(x_{\mathrm{n}}^{\mathrm{p}}\right)^{1/2}x_{\mathrm{s}}^{\mathrm{p}} \tag{4}$$

where $K_{\mathrm{s}}$ is the tangential stiffness coefficient between two contacting particles, and can be written as $K_{\mathrm{s}} = 8G^*\sqrt{R^*}$, here $G^* = \frac{G}{2(1-\nu)}$, $G = \frac{E}{2(1+\nu)}$, $G$ is the shear modulus of granular material. If a particle is in contact with a rigid boundary, the boundary can be set as a sphere with infinite radius. The work is realized by the self-developed program, which is based on CUDA C++.

## 2.2 Setting of granular bed thickness

Since the impact duration is very short when a rigid intruder impacts granular materials, the influence of the shock wave in the granular bed is limited [10]. To reduce the computational time and cost, a finite granular bed with non-reflective boundaries on all but the upper surface can be set up to eliminate boundary effects [42]. Therefore, the propagation distance of the shock wave in the granular bed can be estimated with the dynamic compaction or wave velocity method, and the depth of the granular bed can be determined as [43]:

$$D = \kappa\sqrt{\frac{MH}{10^3}} \tag{5}$$

where $D$ is the maximum depth of the shock wave generated by the intruder in the granular bed; $\kappa$ is the coefficient related to the properties of the granular material with the value in the range of 0.42~0.8, and $\kappa = 0.6$ is taken here; $M$ is the intruder mass; $H$ is the free-falling height of the intruder, which can be deduced from the impact velocity.

To prevent the splashed granular material from scattering on the surface of the intruder during the impact process, a lightweight recessive wall is added above the intruder in the simulation, which has no effect on the dynamic impact. As shown in Fig. 2, the grey solid part represents the actual intruder, while the blue transparent part represents the virtual recessive wall, which is used to prevent the granular media from falling on the top of the intruder. The granular system is generated through a random arrangement of spherical particles. Before simulation, the granular media reaches a physical equilibrium state. The simulation parameters used are listed in Table 1.

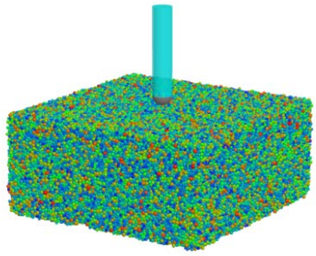

**Fig.2** Impact model

**Table 1** Computational parameters in DEM simulations

| Intruder | | | Granular material | | |
|---|---|---|---|---|---|
| intruder mass | $M$ | 2 kg | particle radius | $r$ | 5~8 mm |
| radius | $R$ | 20 mm | particle bed thickness | $D$ | 0.2 m |
| initial velocity | $v_0$ | 4.0 m/s | particle number | - | 203380 |

### 2.3 Calculation of energy

At each time step, all energies associated with both the intruder and the particles are calculated with special focus on the kinetic energy transferred within the system of particles, while the change of the gravitational energy of granules is negligible.

The kinetic energy of the particles is calculated as follows:

$$E_{\text{granular}} = \sum_{i=1}^{i=N}\left(\frac{1}{2}m_i v_i^2(t) + \frac{1}{2}I_i\omega_i^2(t)\right) \tag{6}$$

The mechanical energy of the intruder is calculated as follows:

$$E_{\text{intruder}} = \frac{1}{2}Mv^2(t) - Mgz \tag{7}$$

## 3. Analysis of impact energy dispersion of granular material

The impact process involves two processes: the initial impact of the intruder on the granular media, and the subsequent collision between the particles. During the first stage, the intruder imparts energy to the granular system, while during the second stage, this energy is dissipated through various interactions between the particles, until the impact system reaches a state of dynamic equilibrium. However, accurately modelling the energy dissipation in real granular systems remains a challenging task, and there is currently no consensus on the most appropriate contact model to be used in the DEM [44]. In particular, traditional numerical models of granular materials do not take into account various forms of energy dissipation, such as contact attrition, local granular breakage, heat energy dissipations or high-frequency wave propagation [45,46]. The interaction force model only includes energy dissipation through frictional processes. No additional viscous or inertial damping are introduced to dissipate energy in the simulations [47], while the assumption is made that the energy transfers and dissipation associated with particles rearrangement are predominant compared with other energy dissipation mechanisms.

### 3.1 Shock model validation and process analysis

Upon the impact of the hemispherical intruder onto the granular medium, a dynamic response occurs in the granular system, as shown in Fig. 3. When subjected to an external impact force, the granular material around the intruder will obtain some energy and then transfer the energy to the surrounding granular material, causing the granular media splashes around due to the acquired velocity. Fig. 3 also demonstrates the velocity distribution of the granular medium and its change over time.

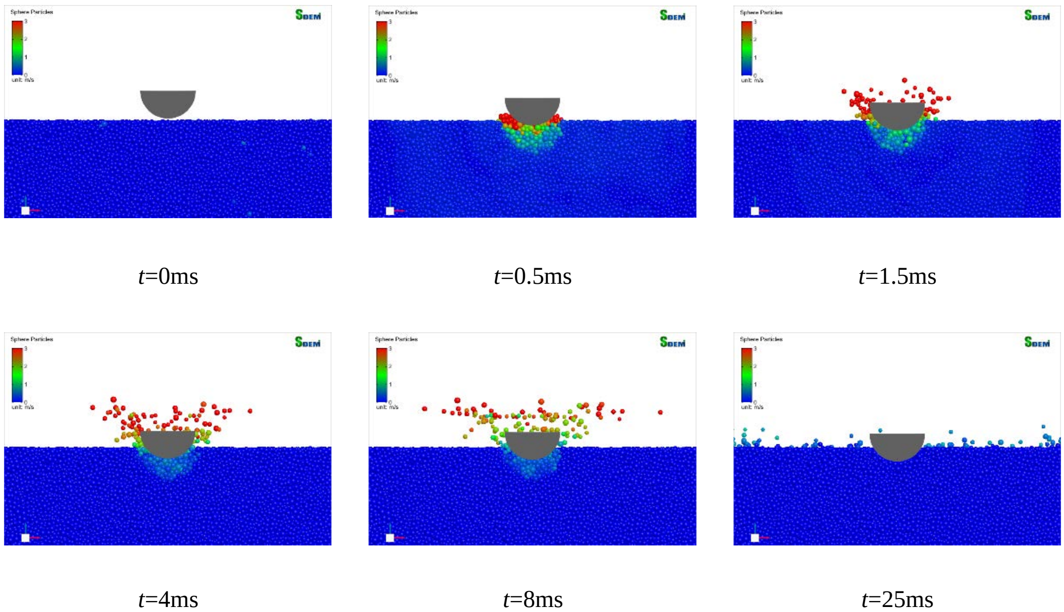


**Fig. 3** Dynamic response of granular media in impact process

When the hemispherical intruder collides with the granular material, it experiences a sudden deceleration due to the strong resistance from the granular particles. Fig. 4 shows the dynamics process for a hemispherical intruder. As illustrated in Fig. 4(a), the maximum penetration depth $z_{\mathrm{stop}}$ is reached shortly after the initial impact. Note that the impact depth z is positive and increases as the intruder penetrates the granular media, with $z = 0$ at $t = 0$. The velocity of the intruder is also shown in Fig. 4 (b): the velocity drops rapidly within 10ms and approaches to zero. From the velocity curve, the stopping time $t_{\mathrm{stop}}$ is determined as the time from the initial contact with the granular media to the time the velocity first reaches zero. The numerical simulation results obtained by DEM with consistent computational parameters are compared with experimental data from Clark and Behringer [48], and found to be in good agreement, demonstrating the reliability of the numerical model. The slight difference may be due to the smoothing of the test results after filtering, and the fluctuation of the simulation results may also be caused by the discontinuity of the granular materials.

In Fig. 5(a), the resistance force applied by the granular media exerted on the intruder is shown. Three peaks appear within 10ms of the impact, gradually decreasing over time. The fluctuation in the resistance force is due to the intermittent release of energy. Fig. 5 (b) illustrates the energy change of the intruder during the impact. Within the first 10ms of the impact, the energy of the intruder rapidly releases, reaching almost zero.

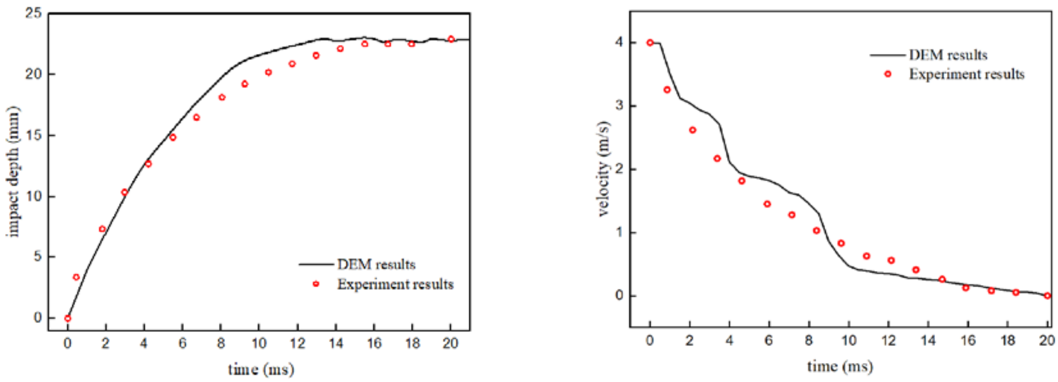


(a) Time history curves of displacement of the hemispherical intruders during impact

(b) Time history curves of velocity of the hemispherical intruders during impact

**Fig. 4** Time history curves of displacement and velocity of the hemispherical intruders during impact and comparison with experimental results [48].

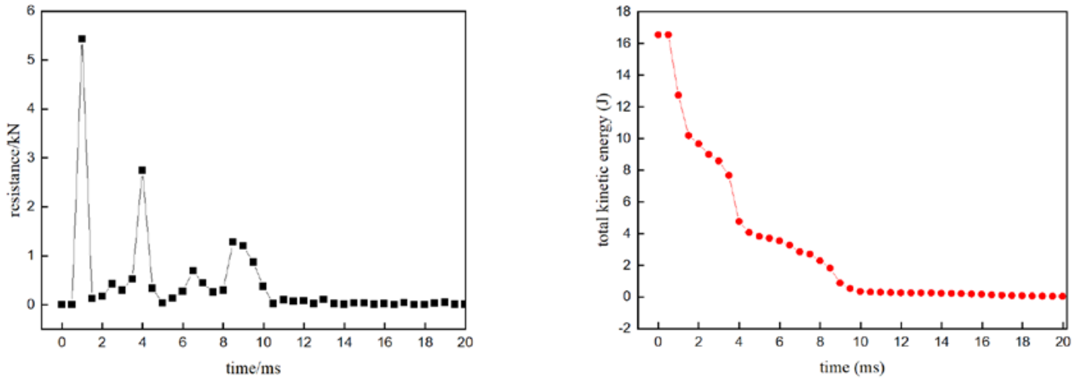


(a) Resistance (b) Total kinetic energy of intruder

**Fig. 5** Time history curves of resistance, total kinetic energy of the hemispherical intruder during impact

## 3.2 Energy transfer between the intruder and the particles

The kinetic energy of the intruder is transferred to the granular media by momentum transfer. The collision between the intruder and the granular media is decomposed into radial and tangential directions along within the granular media. However, the friction coefficient between the intruder and the granular media does not affect the velocity of the intruder during impact, as shown in Fig. 6. This demonstrates that the friction between the intruder and the granular media is unimportant in the momentum transfer process. The tangential momentum between granular materials and the intruder is generated by friction, which leads to the conclusion that the tangential momentum transfer can be neglected. That is, the collision between the intruder and the granular media occurs only in the radial direction. Therefore, the interaction between the intruders and granular materials is established, as shown in Fig. 7.

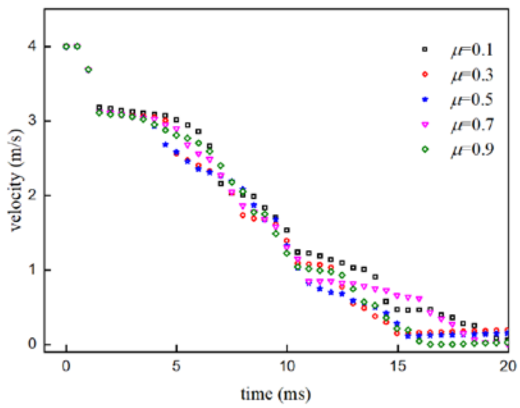


**Fig.6** The influence of friction coefficient between intruder and granular media on impact process

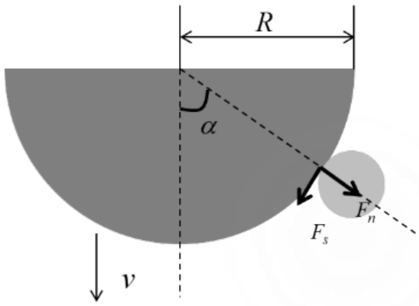


**Fig. 7** Diagram of interaction between a particle and the intruder

The resistance experienced by an intruder during impact is proportional to the square of its velocity, and the proportionality coefficient depends on the dynamic response of the intruder [18]. The momentum transfer and collision time during the collision can be expressed as

$$\Delta p = (1+e)\frac{m_g M}{m_g + M} v\cos\alpha \tag{8}$$

$$\Delta t = \frac{2\mathrm{r}}{v\cos\alpha} \tag{9}$$

where $e$ is the coefficient of restitution between granular materials and the intruder, $m_g$ is the mass of a single particle, $v$ is the impact velocity, $\alpha$ is the angle between the normal direction and the velocity at the collision point, and $r$ is the radius of the particle. The average collision force can be expressed as [28]:

$$f = \frac{\Delta p}{\Delta t} = \frac{(1+e)v^2\cos^2\alpha}{2r}\frac{m_g M}{m_g + M} \tag{10}$$

As $M \gg m_g$, so $\frac{m_g M}{m_g + M} \approx m_g$. The number of particles in contact with the intruder surface can be estimated as $N = k\mathrm{d}S/r^2$, where $k$ represents the contact coefficient and d$S$ denotes the contact area. Accordingly, the total force exerted on the intruder during impact can be expressed as:

$$F = \int fN = \int \frac{(1+e)kv^2\cos^2\alpha}{2r^3} m_g \mathrm{d}S \tag{11}$$

Therefore, the total kinetic energy transferred from the intruder to the particles can be written as:

$$E_k = F2\mathrm{r} = \int 2rfN = \int \frac{(1+e)kv^2\cos^2\alpha}{r^2} m_g \mathrm{d}S \tag{12}$$

The intruder's kinetic energy overall change during impact is shown in Fig. 8. Because the intruder with a larger radius is more likely to contact with the granular media, the efficiency of kinetic energy transfer is improved. Fig. 8(a) shows that the energy of the intruder decreases more rapidly in the initial stage, indicating that a higher impact velocity is beneficial to the energy transfer, which is confirmed in Fig. 8(b). However, the transfer efficiency between the intruder and the granular material approaches almost zero as the velocity reaches a certain value.

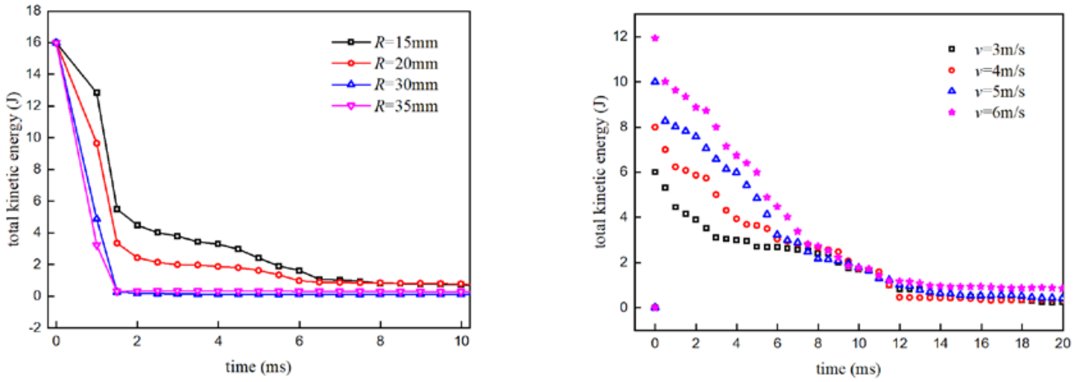


(a) Total kinetic energy of intruder with different size as a function of time

(b) Total kinetic energy of intruder with different velocity as a function of time

**Fig.8** Total kinetic energy of intruder with different size and velocity as a function of time

The dynamic resistance of the intruder is related to the velocity and size of the intruder. As the probability of collision between the granular media and the intruder remains constant, the contact area of the intruder in the hemisphere can be defined as:

$$S_{\text{hemisphere}} = \xi 2\pi R z \tag{13}$$

where $z = z(R, v_0, t)$, $\xi$ is the contact coefficient. So the contact area of the hemispherical intruder can be expressed as:

$$S_{\text{hemisphere}} = \xi 2\pi R z(R, v_0, t) \tag{14}$$

When the impact velocity and radii are changed, the impact depth and contact area change with time as shown in Fig. 9. The contact area is determined by both the impact depth and the size of the intruder. Compared Fig. 9 (a) with Fig. 9 (c), it is found that a larger intruder radius results in a deeper impact depth but a smaller total contact area, highlighting the dominant role of intruder size over impact depth. Compared Fig. 9 (b) with Fig. 9 (d), it is found that changes in impact depth and contact area are similar when the impact velocity is altered, indicating that impact velocity is the major factor affecting the impact depth and consequently the contact area. In summary, increasing the size and initial impact velocity of the intruder is favorable for expanding the contact area between the intruder and the granular media.

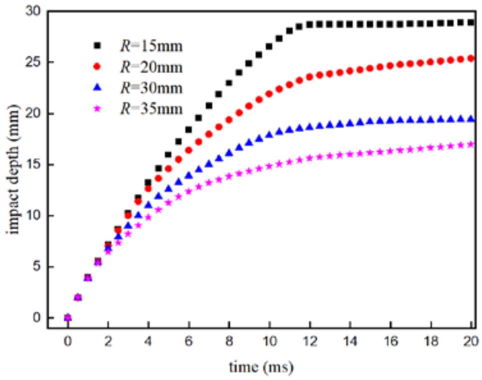


(a) Influences of intruder sizes on impact depth

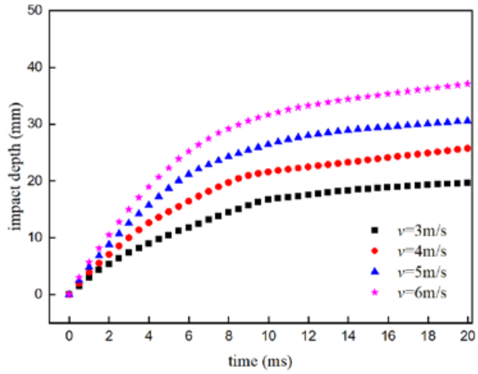


(b) Influences of impact velocity on impact depth

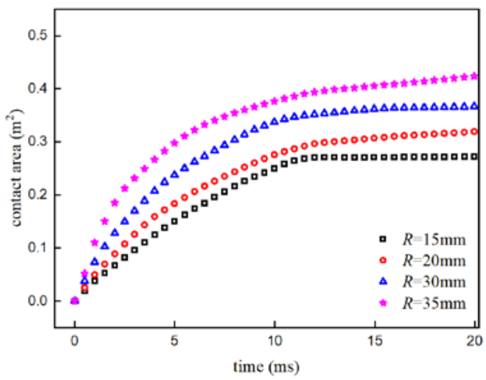


(c) Contact area during the impact as a function of time for different sizes intruders

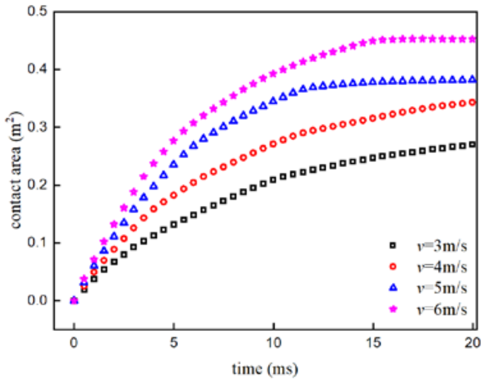


(d) Contact area as a function of time for different impact velocities

**Fig.9** Time history curves of impact depth and contact area under different radius and impact velocities

## 3.3 Influence of intruder shape on the impact process

The resistance of the intruder experienced has no dependence on its shape in the quasi-static impact, which has been verified in previous studies [11,49,50]. However, to explore the relationship between the impact depth and intruder shape during dynamic impact, Clark used triangular-nosed intruders to study the influence of shape by varying the size of the nose [28]. The advantage of this approach is that quantitative relationships can be obtained. However, the use of triangular-nosed intruders does not include all form of contacts. Thus, cylindrical, hemispherical and conical intruders are also used to investigate this issue [51]. They represent plane, surface and point contact, respectively, as shown in Fig. 10. Fig. 11

describes the schematic diagram of the interaction between granular material and intruders with different shapes during impact, where contact occurs only on the surface of the intruder.

(a) cylinder (b) hemisphere (c) cone

**Fig.10** Cylindrical, hemispherical and conical intruders used. They represent plane contact, surface contact and point contact, respectively.

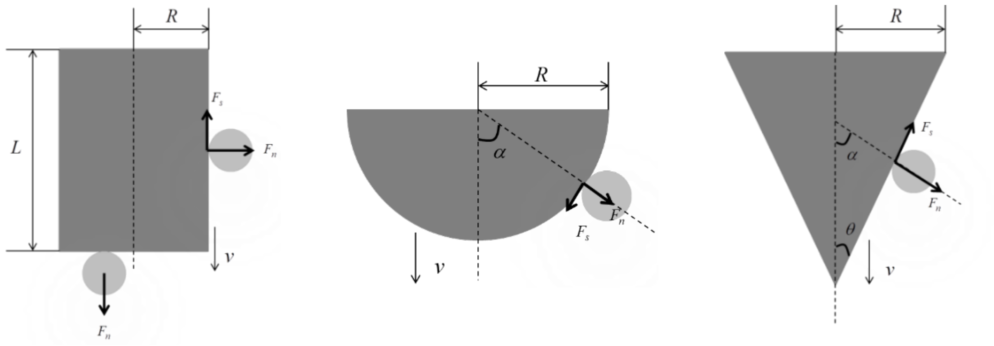


(a) cylinder (b) hemisphere (c) cone

**Fig. 11** Diagram of interaction between granular material and intruder with different shapes

Fig. 12 compares the dynamic responses of three different shaped intruders during impact. At the same time, the dynamic response of the granular medium under impact can also be seen. When the granular media is subjected to the external impact force, the granular material around the intruder will obtain a certain amount of energy which is subsequently transferred to the surrounding granular material. Therefore, the granular media splashes around the impact region.

The contact area of the intruder with cylinder and cone shapes are defined:

$$S_{\text{cylinder}} = \pi R^2 + 2\pi R z \tag{15}$$

$$S_{\text{cone}} = \frac{\pi z^2}{\tan\theta}\sqrt{1 + \frac{1}{\tan^2\theta}} \tag{16}$$

The maximum impact depths of the three shapes under different initial impact energies are shown in Fig. 13. The impact depth increases with the increase of the impact energy. As expected, it has:

$$z_{\text{stop}}(\text{cylinder}) < z_{\text{stop}}(\text{hemisphere}) < z_{\text{stop}}(\text{cone}) \tag{17}$$

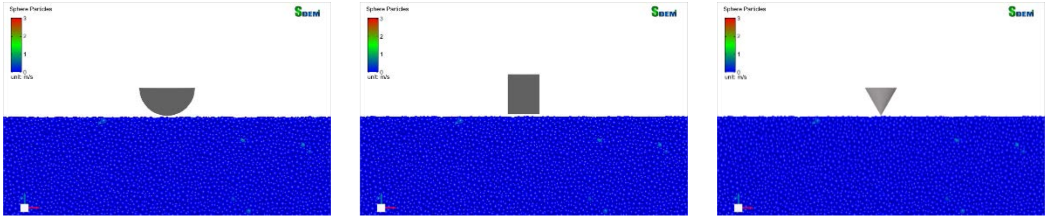

*t*=0ms

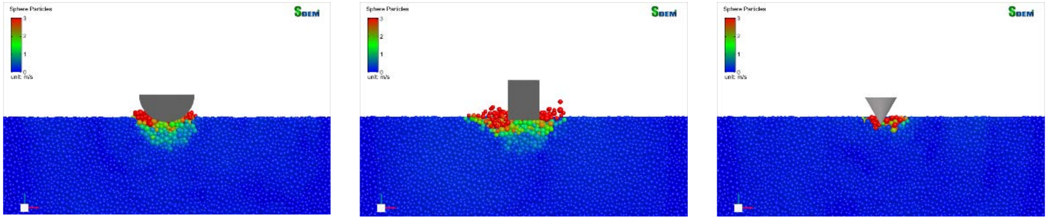

*t*=0.5ms

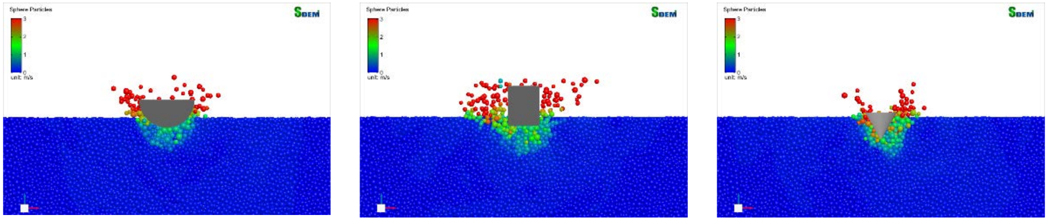

*t*=1.5ms

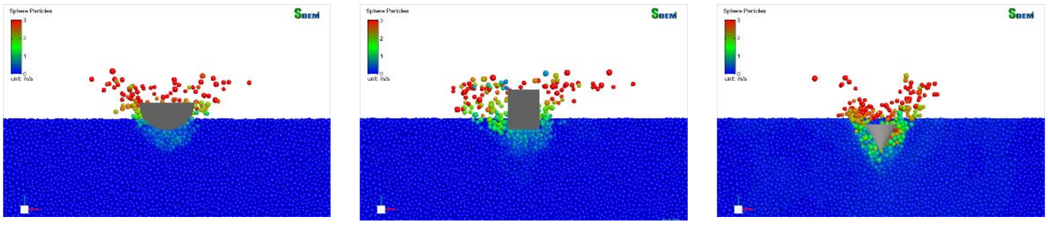

*t*=4ms

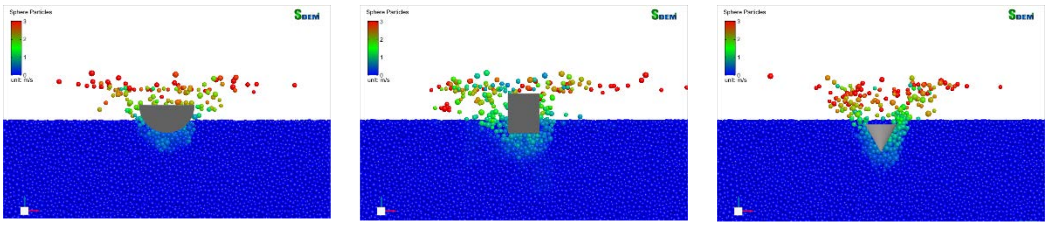

*t*=8ms

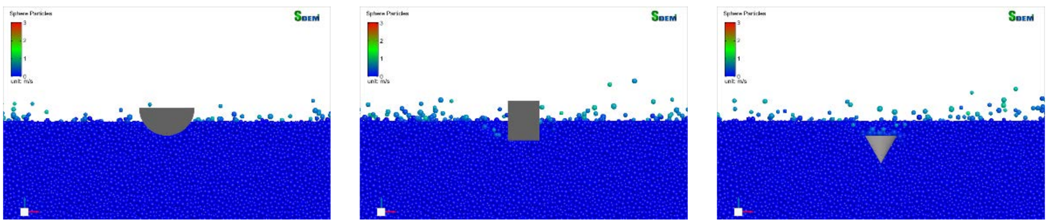

*t*=25ms

**Fig. 12** Dynamic response of granular media in impact process

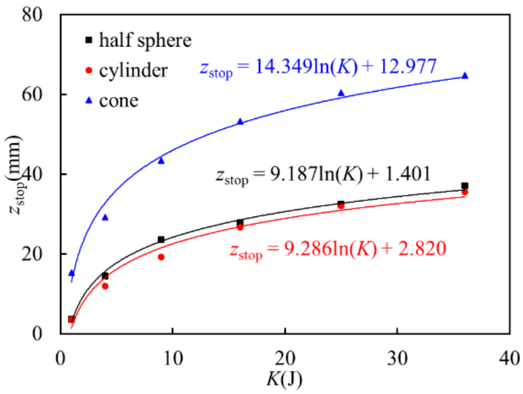


**Fig. 13** The relationship between maximum impact depth and different impact energies in different shapes intruders

The impact depth of the intruder with a sharper contact point is greater. The initial impact energy can be written as $K = \frac{1}{2}Mv^2$ and $\frac{\mathrm{d}K}{\mathrm{d}z} = Ma$. Therefore, the following expressions can be obtained:

$$\frac{\mathrm{d}K}{\mathrm{d}z} = Mg - \beta(z) - \frac{2h(z)}{M}K \tag{18}$$

This is a first-order ordinary differential equation with non-constant coefficients, making it an inhomogeneous ODE. Standard techniques for solving such equations can apply to obtain a formal solution for $K(z)$:

$$K(z) = K_{\mathrm{p}}(z)(K_0 + \varphi(z)) \tag{19}$$

where $K_0$ is the initial kinetic energy of the intruder.

$$K_{\mathrm{p}}(z) = e^{\left(-\int_0^z \frac{2}{M} h(z')\mathrm{d}z'\right)} \tag{20}$$

$$\varphi(z) = \int_0^z \frac{Mg - \beta z'}{K_{\mathrm{p}}(z')}\mathrm{d}z' \tag{21}$$

In order to get the relationship between the impact depth $Z_{\mathrm{stop}}$ and $K$, it is usually assumed that the drag coefficient is constant, i.e. $h(z) = \chi h$, $\beta(z) = \beta$. Therefore, it is possible to find the stopping distance by setting $K(Z_{\mathrm{stop}}) = 0$, i.e.

$$Z_{\mathrm{stop}} = \frac{M}{2\chi}\ln\left[1 + \frac{2\chi K}{M(\beta - Mg)}\right] \tag{22}$$

Fig. 13 presents the fitted curves that reveal the relationship between the intruder shape and the values of $\chi$ and $\beta$, which determine the impact depth. It is evident from the graph that the values of $\chi$ and $\beta$ vary with the intruder shape, highlighting the impact depth's dependency on the intruder shape. These findings are consistent with the results of photoelastic experiments [48]. According to Eq. (22), the depth is proportional to the logarithmic value of kinetic energy, while Eqs. (14)-(16) reveal that the contact area is at least a function of the radius. This explains why the radius has a significant impact on the contact area.

### 3.4 Analysis of energy dissipation mechanism of particles

Granular materials have the characteristic of energy dissipation [52,53]. When the energy is transferred from the intruder to the granular media, strong extrusion and friction occur between the particles, resulting in a complex internal force chain structure that constantly breaks and reorganizes, thereby consuming a significant amount of energy [54,55]. Due to the viscous effect and plastic deformation between particles, irreversible energy is also absorbed [56]. In granular systems, contact forces are transmitted through force chains, which cause the impact load expand continuously in space and reduces its strength. Furthermore, the force chain has a significant time effect on the process of force propagation, which delays the instantaneous impact load in time and plays a buffering role [57].

In addition, the intruder loses most of its energy at the moment of contact with the granular media. However, during deep impacts, the granular media undergoes significant displacement, resulting in increased compression and shear deformation, which is a highly dissipative phenomenon. This deformation is mainly caused by the friction and volume changes that occur as granular material slides, rolls, and climbs [58,59]. The high average stress in front of the intruder leads to increased friction force between the particles, while the volume changes that occur during shear result in pressure evolution and energy dissipation. In some cases, the locally high stress can lead to granular rupture or even complete crushing [60], resulting in new surface area and additional energy dissipation. Although this paper does not consider the energy dissipation resulting from granular rupture, it is an important part of the actual impact process. These microscopic and mesoscale dissipation mechanisms provide a foundation for understanding the intruder impact in granular media.

As an example, the impact dynamics of a hemispherical intruder is examined by analyzing the energy distribution of the system throughout the impact process, as shown in Fig. 14. The energy distribution is divided into three components: the mechanical energy of the intruder (red curve), the potential and kinetic energy of the granular media (pink curve), and the energy dissipated during the impact (blue curve). The pink curve rapidly increases from zero at the initial time, then gradually decreases to zero, while the red curve decreases from its maximum value to zero. The energy dissipated by the system is represented by the blue curve. The total energy of the system $E$ can be expressed as:

$$E = E_{\mathrm{granular}} + E_{\mathrm{intruder}} + E_{\mathrm{dissipation}} \tag{23}$$

where $E_{\mathrm{granular}}$ and $E_{\mathrm{intruder}}$ are the mechanical energy of the granular media and the intruder, respectively. $E_{\mathrm{dissipation}}$ is the energy currently dissipated by the impact system. The formula presented above represents the fundamental law of energy conservation. At the beginning of the impact process, the total energy of the system is primarily determined by the mechanical energy of the intruder. However, a crucial turning point occurs at the black dotted line. Beyond this point, the granular media becomes the primary energy carrier after colliding with the intruder and receiving its mechanical energy. As a result of friction and collision between the granular particles, the mechanical energy is gradually converted into other forms of energy. The mechanical energy of the system decreases over time, ultimately reaching a stable state during the dynamic response.

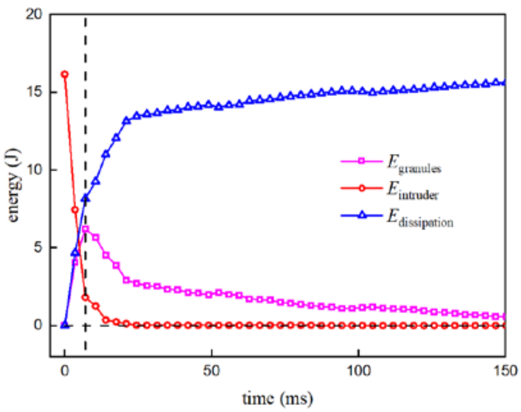


**Fig. 14** The energy distribution of the impact system

Fig. 15 shows that the larger the initial impact energy of the intruder, the more energy $E_{\mathrm{granular}}$ the granular system obtains, the longer the dissipation time $T$, and the larger the proportion of the granular material involved in energy dissipation $\gamma$. The relationship of these three quantities can be expressed as:

$$T\gamma = \zeta \ln E_{\mathrm{granular}} + c \tag{24}$$

where $\zeta$ and $c$ are coefficients related to the physical properties of the granular material. The determination of these coefficients is an important aspect that will be addressed in future work.

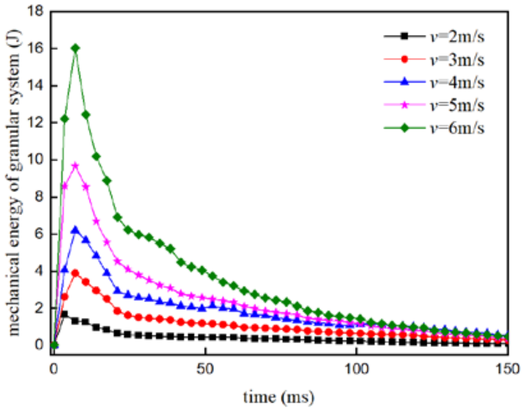


(a) The change of mechanical energy of granular system with time under different impact velocities

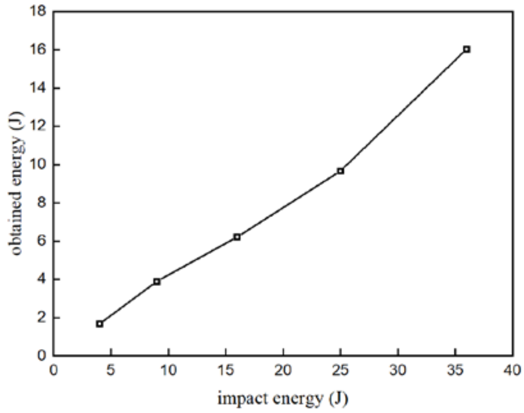


(b) Maximum energy possessed by a granular system at different impact energies

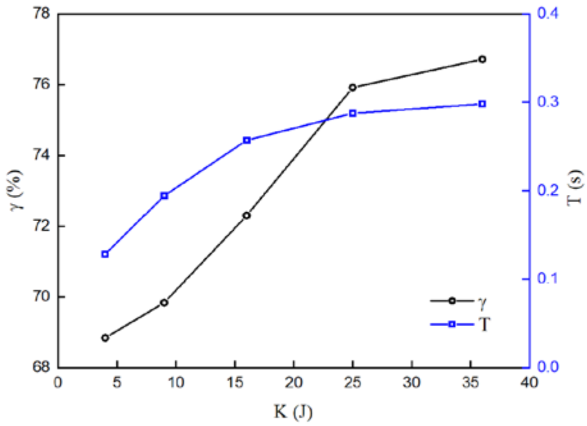


(c) The black line is the proportion of the largest number of granular materials participating in the dissipation, and the blue line is the total dissipation time

**Fig. 15** Effect of initial mechanical energy of impact system on dissipation process

## 4. Conclusions

Based on the empirical formula of impact dynamics, a numerical simulation model is set up in this paper. The dynamic impact is decomposed into two main processes, that is, the energy transfer from the intruder to the granular media and the energy dissipation by collision between particles. The analysis shows that friction between the granular materials and the intruder plays a negligible role in momentum transfer during the impact. In addition, the influence of the contact area on the mechanical energy transfer process is analyzed. It is found that the intruder size plays a dominant role in determining the contact area, and that the depth only affects its development trend. Further research shows that the factors affecting the impact depth include impact velocity and intruder shape. The dynamic impact is strongly dependent on the intruder shape, specifically on the coefficient of the inertial force term. More research is needed to quantify the shape parameters and derive more general rules. The study also found that when the granular system is large enough, the initial impact energy determines the proportion of the granular material involved in energy dissipation and the dissipation time, and there is a certain quantitative relationship among them. The coefficients involved are related to the physical properties of the granular media. The current study also provides a further understanding of the buffer energy dissipation properties of granular materials, which will be valuable for applications in space landing, exploration and recovery.

## Declaration of Competing Interest

The authors declare that they have no known competing financial interests or personal relationships that could have appeared to influence the work reported in this paper.

## Acknowledgments

This study is financially supported by the National Natural Science Foundation of China (Grant Nos. 12072217 and 12102294).

## References

[1] Su Y, Cui Y, Ng C W W, Choi C E, Kwan J S H. Effects of particle size and cushioning thickness on the performance of rock-filled gabions used in protection against boulder impact. Canadian Geotechnical

Journal, 2019, 56(2): 198–207.

[2] Fang J, Wang L, Hong Y, Zhao J. Influence of solid-fluid interaction on impact dynamics against rigid barrier: CFD-DEM modeling. Géotechnique, 2022, 72(5): 391-406.

[3] Ji S, Liang S. DEM-FEM-MBD coupling analysis of landing process of lunar lander considering landing mode and buffering mechanism. Advances in Space Research, 2021, 68: 1627–1643.

[4] Wang Z, Ma D, Suo T, Li Y, Manes A. Investigation into different numerical methods in predicting the response of aluminosilicate glass under quasi-static and impact loading conditions. International Journal of Mechanical Sciences, 2021, 196: 106286.

[5] Zhang R, Zhao X, Zhao G, Dong S, Liu H. Analysis of solid particle erosion in direct impact tests using the discrete element method. Powder Technology, 2021, 383: 256-269.

[6] Pacheco-Vazquez F, Ruiz-Suarez J C. Cooperative dynamics in the penetration of a group of intruders in a granular medium. Nature Communication, 2010, 1(123): 1-7.

[7] Liu X, Jiao T, Liu X, Ma L, Su J, Chen W, Sun Q, Huang D. Rectification effect on solitary waves in the symmetric Y-shaped granular chain. Granular Matter, 2017, 19(3): 55.

[8] Ciamarra M P, Lara A H, Lee A T. Dynamics of drag and force distributions for projectile impact in a granular medium. Physical Review Letters, 2004, 92(19): 194301.

[9] Umbanhowar P, Goldman D I. Granular impact and the critical packing state. Physical Review Letters, 2010, 82(1): 010301.

[10] Seguin A, Bertho Y, Gondret P. Influence of confinement on granular penetration by impact. Physical Review E, 2008, 78(1): 010301–010304.

[11] Liang S, Liu L, Ji S. DEM Simulations of Resistance of Particle to Intruders During Quasistatic Penetration. Computer Modeling in Engineering & Sciences, 2021, 128(1): 145-160.

[12] Guo J. Exact solution for depth of impact crater into granular bed. Journal of Engineering Mechanics, 2018, 144(1): 06017018.

[13] Ye X, Wang D, Zheng X. Influence of particle rotation on the oblique penetration in granular media. Physical Review E, 2012, 86(6): 061304-061315.

[14] Kann S V, Joubaud S, Caballerorobledo G A, Lohse D, Meer D. The effect of finite container size on granular jet formation. Physical Review E, 2010, 81(4): 041306-041320.

[15] Royer J R, Corwin E I, Eng P J, Jaeger H M. Gas-mediated impact dynamics in fine-grained granular materials. Physical Review Letters, 2007, 99(3): 038003–038006.

[16] Omidvar M, Iskander M, Bless S. Response of granular media to rapid penetration. International Journal of Impact Engineering, 2014, 66: 60-82.

[17] Jayasundara C T, Zhu H P. Impact energy of particles in ball mills based on DEM simulations and data-driven approach. Powder Technology, 2022, 395: 226-234.

[18] Bester C S, Behringer R P. Collisional model of the drag force of granular impact. European Physical Journal, 2017, 140: 03017.

[19] Uehara J S, Ambroso M A, Ojha R P, Durian D J. Low-speed impact craters in loose granular media. Physical Review Letters, 2003, 90(19): 194301–194305.

[20] Han E, Peters I R, Jaeger H M. High-speed ultrasound imaging in dense suspensions reveals impact-activated solidification due to dynamic shear jamming. Nature Communication, 2016, 7: 12243–12250.

[21] Wang J, Chu X, Jiang Q, Xiu C. Energy transfer and influence of excitation frequency in granular materials from the perspective of Fourier transform. Powder Technology, 2019, 356: 493-499.

[22] Wang J, Chu X, Zhang J, Liu H. The effects of microstructure on wave velocity and wavefront in granular assemblies with binary-sized particles. International Journal of Solids and Structures, 2019, 159: 156-162.

[23] Xiu C, Chu X, Wan J, Wang J. Numerical simulation of impulse waves in Cosserat media based on a time‐discontinuous Galerkin finite element method. International Journal for Numerical Methods in Engineering, 2021, 122(17): 4507-4540.

[24] Royer J R, Conyers B, Corwin E I, Eng P J, Jaeger H M. The role of interstitial gas in determining the impact response of granular beds. Europhysics Letters, 2011, 93(2): 28008.

[25] Ambroso M A, Santore C R, Abate A R, Durian D J. Penetration depth for shallow impact cratering. Physical Review E, 2004, 71(5): 051305–051311.

[26] Goldman D I, Umbanhowar P. Scaling and dynamics of sphere and disk impact into granular media. Physical Review E, 2008, 77(2): 021308–021311.

[27] Clark A H, Petersen A J, Kondic L, Behringer R P. Nonlinear force propagation during granular impact. Physical Review Letters, 2015, 114(14): 1-5.

[28] Clark A H, Petersen A J, Behringer R P. Collisional model for granular impact dynamics. Physical Review E, 2014, 89(1): 012201-012212.

[29] Amato J C, Williams R E. Crater formation in the laboratory an introductory experiment in error analysis. American Journal of Physics, 1998, 66(2): 141-143.

[30] De Bruyn J R, Walsh A M. Penetration of spheres into loose granular media. Canadian Journal of Physics, 2004, 82(6): 439-446.

[31] Wang C, Deng A, Taheri A, Zhao H H, Li J. Modelling particle kinetic behaviour considering asperity contact: formulation and DEM simulations. Granular Matter 2019, 21(2): 16-31.

[32] Liang S, Ji S. Coordinated time-stepping method for coupled DEM-FEM-MBD algorithm. International Journal of Computational Methods, 2022, 19(03): 2150067.

[33] Du Y, Wang S, Zhang J. Energy dissipation in collision of two balls covered by fine particles. International

Journal of Impact Engineering, 2010, 37(3): 309-316.

[34] Katsuragi H, Durian D J. Drag force scaling for penetration into granular media. Physical Review E, 2013, 87(5): 052208-052212.

[35] Li Y, Dove A, Curtis J S, Colwell J E. 3D DEM simulations and experiments exploring low-velocity projectile impacts into a granular bed. Powder Technology, 2016, 288: 303–314.

[36] Liu J, Bosco E, Liu J, Suiker A S J. Multi-scale modelling of granular materials: numerical framework and study on micro-structural features. Computational Mechanics, 2018, 63(2): 409-427.

[37] Schulz D, Woschny N, Schmidt E, Kruggel-Emden H. Modelling of the detachment of adhesive dust particles during bulk solid particle impact to enhance dust detachment functions. Powder Technology, 2022, 400: 117238.

[38] Yang D, Chu X, Xiu C, Pan Y. Influence of Aspect Ratio on Wave Propagation in Granular Crystals Consisting of Ellipse-Shaped Particles International Journal of Applied Mechanics, 2022, 15(01): 2250096.

[39] Ji S, Di S, Liu S. Analysis of ice load on conical structure with discrete element method. Engineering Computations, 2015, 32(4): 1121-1134.

[40] Ramírez R, Pöschel T, Brilliantov N V, Schwager T. Coefficient of restitution of colliding viscoelastic spheres. Physical review E, 1999, 60(4): 4465.

[41] Bahaaddini M, Sharrock G, Hebblewhite B K. Numerical direct shear tests to model the shear behaviour of rock joints. Computers and Geotechnics, 2013, 51: 101–115.

[42] Newhall K A, Durian D J. Projectile-shape dependence of impact craters in loose granular media. Physical Review Letters, 2003, 68(6): 060301.

[43] Wu X, Zhong S, Ling D, Chen Y. Model test study of vertical impact of space lander footpad. Rock and Soil Mechanics, 2012, 33(4): 1045–1050.

[44] Antypov D, Elliott J A, Hancock B C. Effect of particle size on energy dissipation in viscoelastic granular collisions. Physical Review E, 2011, 84(2): 021303.

[45] Metzger M J, Glasser B J. Simulation of the breakage of bonded agglomerates in a ball mill. Powder Technology, 2013, 237: 286-302.

[46] Bourrier F, Nicot F, Darve F. Evolution of the micromechanical properties of impacted granular materials. Comptes Rendus Mécanique, 2010, 338: 639-647.

[47] Mitarai N, Nakanishi H. Velocity correlations in dense granular shear flows: effects on energy dissipation and normal stress. Physical Review E, 2007, 75(3): 031305.

[48] Clark A H, Behringer R P. Granular impact model as an energy-depth relation. Europhysics Letters, 2013, 101(6): 64001–64007.

[49] Katsuragi H, Durian D J. Unified force law for granular impact cratering. Nature Physics, 2007, 3(6): 420423.

[50] Kang W, Feng Y, Liu C, Blumenfeld R. Archimedes' law explains penetration of solids into granular media. Nature Communication, 2018, 9: 1101–1109.

[51] Brzinski T A, Mayor P, Durian D J. Depth-dependent resistance of granular media to vertical penetration. Physical Review Letters, 2013, 111(16): 168002–168008.

[52] Pacheco-Vazquez F, Caballero-Robledo G A, Solano-Altamirano J M, Altshuler E, Batista-Leyva A J, Ruiz-Suarez J C. Infinite penetration of a projectile into a granular medium. Physical Review Letters, 2011, 106(21): 218001-218004.

[53] Mwangi F M, Kanny K. Development of granular-medium-based impact energy management system. International Journal of Crashworthiness, 2012, 17(4): 401-414.

[54] Ma L, Huang D, Chen W, Jiao T, Sun M, Hu F, Su J. Oscillating collision of the granular chain on static

wall. Physics Letters A, 2017, 381(5): 542–548.

[55] Chou S H, Yang S J, Hsiau S S. Investigation on the erosion and deposition process of granular collapse flow on an erodible inclined plane. Powder Technology, 2023, 414: 118086.

[56] Clark A H, Kondic L, Behringer R P. Particle scale dynamics in granular impact. Physical Review Letters, 2012, 109(23): 238302.

[57] Lydon J, Theocharis G, Daraio C. Nonlinear resonances and energy transfer in finite granular chains. Physical Review E, 2015, 91(2): 023208.

[58] Tabuteau H, Sikorski D, De Vet S J, De Bruyn J R. Impact of spherical projectiles into a viscoplastic fluid. Physical Review Letters, 2011, 84(3): 031403.

[59] Kondic L, Fang X, Losert W, O'hern C S, Behringer R P. Microstructure evolution during impact on granular matter. Physical Review Letters, 2012, 85(1): 011305.

[60] Denisov D V, Lorincz K A, Uhl J T, Dahmen K A, Schall P. Universality of slip avalanches in flowing granular matter. Nature Communication, 2016, 7: 10641.